Yavuzcanli, M., Alpaslan, D., Turan, A., & Ersen Dudu, T. (2025). *Journal of the Turkish Chemical Society Section B: Chemical Engineering*, *8*(2), 185–202.

Biomedical Potential of p(Rt) Particles Synthesized from Rubia Tinctorum L. Extract: Characterization, Bioactivity and Controlled Drug Release

Mustafa Yavuzcanli [a], Duygu Alpaslan [a*], Abdullah Turan [b], Tuba Ersen Dudu [a]

[a]Van Yüzüncü Yıl University, Institute of Natural and Applied Science, Department of Chemical Engineering, Van 65080, Türkiye.
[b]Van Yüzüncü Yıl University, Science Faculty, Department of Molecular Biology and Genetic, Campus, Van 65080, Türkiye

Abstract: *Rubia tinctorum L. (*Root Dye, Madder*)* has been historically used in textile dyeing and is valued for its natural antibacterial, antioxidant, and therapeutic properties. In this study, the synthesis of poly(Rubia tinctorum) (p(Rt)) particles from Rubia tinctorum L. extract and their biomedical applications are reported for the first time. The extract and synthesized particles were characterized using SEM, FTIR, DLS, zeta potential analysis, and HPLC. The bioactivity of p(Rt) particles, including antimicrobial, antioxidant, and biocompatibility properties, were assessed. Drug release studies showed significant paracetamol and ceftriaxone release at different pH levels, with release kinetics fitting the Korsmeyer-Peppas model. This study highlights the novelty of p(Rt) particles and their potential in biomedical applications, particularly in drug delivery.

Keywords: Antimicrobial, Antioxidant, Biocompatibility, Drug release, Rubia tinctorum L. (Root Dye).

Submitted: April 23, 2025. **Accepted:** August 21, 2025.

Cite this: Yavuzcanli, M., Alpaslan, D., Turan, A., & Ersen Dudu, T. (2025). Biomedical Potential of p(Rt) Particles Synthesized from Rubia Tinctorum L. Extract: Characterization, Bioactivity and Controlled Drug Release. *Journal of the Turkish Chemical Society Section B: Chemical Engineering*, *8*(2), 185–202. https://doi.org/10.58692/jotcsb.1682389

***Corresponding author. E-mail:** alpaslanduygu@gmail.com

1. INTRODUCTION

Rubia tinctorum L. (commonly known as madder) is a species in the Rubia genus of the Rubiaceae family, historically valued for its vibrant red dye extracted from its roots. (Böhm, 1993) The plant's name originates from the Latin Rubia (red) and tinctorum (to paint). Native to Anatolia and Southeastern Europe, it has been cultivated across the Mediterranean, Asia, and the Caucasus for centuries and is now found in China, Japan, North and South America, and the Malaysian Archipelago (Böhm, 1993).

Beyond its significance in textile dyeing, Rubia tinctorum L. possesses various health, ecological, and economic benefits (Ozdemir and Karadag, 2023). It has been traditionally used for medicinal purposes, including as a diuretic, preventer of renal stones, and antifungal agent. The root extract is rich in anthraquinone (Orbán et al., 2008) derivatives such as alizarin and purpurin (Gilbert and Cooke, 2001), which exhibit anti-inflammatory, antimicrobial, antibacterial, and antidiuretic properties. These bioactive compounds make the plant a promising candidate for biomedical applications (Manojlovic et al., 2005; Marsoul et al., 2023) (Swain, 1966).

Despite its well-documented use in textiles and traditional medicine, the potential of *Rubia tinctorum L.* in advanced biomedical applications remains largely unexplored (Manojlovic et al., 2005). Limited studies have investigated its bioactivity in modern drug delivery systems, and no research has reported the synthesis of poly(*Rubia tinctorum*) (p(Rt)) particles for controlled drug release. This study aims to bridge this gap by examining the biomedical potential of p(Rt) particles synthesized from different extracts of *Rubia tinctorum L.*

This study hypothesizes that p(Rt) particles synthesized from Rubia tinctorum L. extract exhibit significant bioactivity and potential for controlled drug release. The primary objectives are to synthesize p(Rt) particles using ethanol, methanol, and aqueous extracts of Rubia tinctorum L. and to characterize the synthesized particles through SEM, FTIR, DLS, zeta potential analysis, and HPLC. Additionally, this study aims to evaluate the antimicrobial, antioxidant, and biocompatibility properties of p(Rt) particles, as well as to investigate the drug release behavior of paracetamol and ceftriaxone and assess their release kinetics. By addressing these objectives, it seeks to establish a foundation for applying p(Rt) particles in biomedical fields, contributing to both scientific knowledge and the economic value of Rubia tinctorum L.

2. MATERIAL AND METHOD

2.1. Preparation of Rubia tinctorum L Extracts

In this study, the roots of the *Rubia tinctorum L.* plant found in different parts of Turkey were used. *Rubia tinctorum L.* was collected from the Manisa Kırkağaç district. It was dried by local methods and used without any chemical treatment. First, root dye (*Rubia tinctorum L.)* was ground and 1 g was weighed and stirred in 50 mL solvent (pure water, ethanol, and methanol) for 48 hours at 50 °C on a magnetic stirrer. At the end of 48 hours, the solution was taken into falcon tubes and kept for 20 minutes. It was centrifuged at 9000 rpm. After centrifugation, the precipitated solid and the liquid phase was separated. The separated extracts were taken into falcon tubes and kept at +4 °C for analysis.

2.2. High Performance Liquid Chromatography (HPLC) Analysis

Thermo Scientific Brand UltiMate 3000 model High Performance Liquid Chromatography (HPLC) device was used to determine the flavonoid and anthraquinone substances in the *Rubia tinctorum L.* extraction.
HPLC analysis parameters are as follows:
Model: Dionex 3000 U-HPLC (USA)
Column: Waters XTerra MS (4.6 mm x25 mm; 5 µm; C18) Detector: Dionex 3000 U-HPLC Diode array detector (USA)
Mobile phase used for anthraquinone detection in HPLC;
Mobile phase: Acetonitrile(66)-Water(34)
Detection: 254 nm-280 nm
Flow rate: 0.5 mL/min
Column temperature: 35 °C
Injection amount: 20 µL
Mobile phase used for flavonoid detection in HPLC;
Mobile phase A: Methanol(80)Acidic acid(2)-Water(18)
Mobile phase B: Methanol(20)Acidic acid(2)-Water(78)
Detection: 254 nm-280 nm
Flow rate: 0.6 mL/min
Column temperature: 24 °C
Injection amount: 20 µL
Identification of the anthraquinone and phenolic compounds in the sample was made by comparing the retention time of the compounds in the column and the UV-spectra of the respective standard substances and their spectra. The identification of the peaks of the anthraquinone and phenolic compounds and the wavelengths at which the compounds gave the maximum absorbance value were evaluated. For this reason, a wavelength of 254 nm and 280 nm was chosen for the analysis of phenolic compounds.

2.3. Synthesis of poly(Rubia tinctorum L.) (p(Rt)) Particles

Root dye (*Rubia tinctorum L.*) extracts extracted in water, ethanol and methanol were used in experimental studies. Ethylene glycol dimethacrylate (EGDMA) was used as a crosslinking agent

and p(Rt) particles were synthesized by redox polymerization technique in ethanol-water emulsion medium. The reaction was carried out at 50 °C and the particles formed at the end of the polymerization and the substances that did not react with it were removed by washing. The washing process takes 20 minutes with acetone. It was done 3 times at 9000 rpm. After the obtained particles were washed, they were dried in an oven at 40 °C and stored for further studies. Synthesis, schematic presentation of p(Rt) particles was given in Figure 1**.**

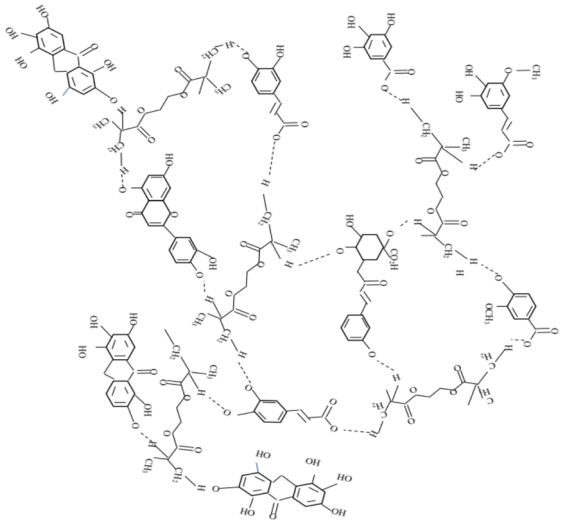

Figure 1. Synthesis, schematic presentation of p(Rt) particles.

The method applied in p(Rt) particle synthesis was also used for drug-loaded p(Rt)-particle synthesis. However, after the crosslinking agent was added to the polymerization mixture, the polymerization reaction was initiated by adding 1 mL of 50 ppm ceftriaxone (antibiotic) or paracetamol (pain reliever) drugs separately. The reaction was carried out at 50 °C and the drug-loaded p(Rt) particles formed at the end of polymerization did not react with the polymerization mixture. The substances were removed by washing, dried, and stored at 4 °C for further studies.

2.4. Characterization of Particles

Fourier Transform Infrared Spectroscopy, SEM Ultra Field Emission-Energy Dissipative Spectroscopy X-ray, Particle size (DLS), and particle charge (zeta potential, Zeta) were used for the characterization of p(Rt) particles.

2.5. Blood Clotting and Hemolysis Analysis

To evaluate the blood clotting (Alpaslan et al., 2021b) and hemolysis analysis (Alpaslan et al., 2022b) methods which were explained in the literature were applied.

2.6. Antioxidant Analysis

The antioxidant properties of the particles were investigated according to Folin-Ciocalteu (Alpaslan et al., 2021c; Singleton and Rossi, 1965) (Alpaslan, 2019; Alpaslan et al., 2018b; Alpaslan et al., 2021a; Childs and Bardsley, 1975) method specified in the literature (Ruch et al., 1989).

2.7. Antimicrobial Analysis

The antimicrobial analysis described in the literature (Alpaslan et al., 2018a; Alpaslan et al., 2020; Korsmeyer et al., 1983) was used to analyze the results. The antimicrobial capacities of $p(Rt)_m$, $p(Rt)_e$ and $p(Rt)_w$ were tested against three Gram (+) (*Staphylococcus aureus, Bacillus cereus, Enterococcus faecalis*), two Gram (-) (*Escherichia coli , Pseudomonas aeruginosa*) bacteria and one yeast (*Candida albicans*).

2.8. Drug Release Studies

The ceftriaxone and paracetamol release capacity of the $p(Rt)_m$, $p(Rt)_e$ and $p(Rt)_w$ particle were measured according to the procedure outlined by Alpaslan et al (Alpaslan et al., 2021c; Olak et al.,

2020). To determine the release kinetics, the most often employed models were zero order (Zm), first order (F), Higuchi (H), and Korsmeyer-Peppas (KP).

3. RESULTS AND DISCUSSION

Within the scope of this study, root dye (*Rubia tinctorum L.)* plant extracts were obtained from three different solvent media: purified water, ethanol and methanol solvents. The plant/solvent ratio, extraction time and temperature were kept constant at 1 g/50 mL, 48 hours and 50 °C, respectively, and mixed continuously using a magnetic stirrer. After the extraction time is completed, the solution is left for 20 min. It was centrifuged at 9000 rpm and the solid and liquid phases were separated to obtain Rubia tinctorum L. extract. The obtained extracts were crosslinked by redox polymerization technique in ethanol-water emulsion medium using Ethylene glycol dimethylacrylate (EGDMA) crosslinker. With this method of synthesis, 3 different p(Rt) particles were synthesized and named as $p(Rt)_m$, $p(Rt)_e$ and $p(Rt)_w$. At the same time, $p(Rt)_m$, $p(Rt)_e$ and $p(Rt)_w$ paracetamol, and ceftriaxone drug-loaded particles were synthesized during particle synthesis. Structural characterization of the obtained Rt extract and p(Rt) particles was performed with Scanning Electron Microscopy (SEM), Fourier Transform-Infrared (FTIR), High Performance Liquid Chromatography (HPLC), Particle size (DLS), and particle charge (zeta potential, Zeta) analysis, and their bioactivity (antimicrobial, antioxidant, and biocompatibility) properties and drug release behaviors were also investigated.

3.1. High-Performance Liquid Chromatography (HPLC)

The contents of the compounds found in *Rubia tinctorum* L. cultivars can differ significantly between different species (Essaidi et al., 2017; Marhoume et al., 2021b) (Derksen et al., 2021; Zohra et al., 2022). In Figure 2 and 3, in HPLC chromatograms of *Rubia tinctorum L.* extracts, lucidin primeveroside (1), ruberythric acid (2), pseudo purpurin (3), lucidin (4), alizarin (5), purpurin (6), anthraquinone components and gallic acid (1), protocatechuic acid (2), syringic acid (3), chlorogenic acid (4), caffeic acid (5), ferulic acid (6), Rutin (7), vanillic (8), seinamic acid (9) and quercetin (10) flavonoid compound seen. In some studies, 36 anthraquinones were detected in the root shoots of the root dye (*Rubia tinctorum L.*) plant.

The HPLC analysis results of the anthraquinone contents in three different Rt extracts reveal notable differences in their composition. As shown in Figure 3, the water extract contains a significantly higher amount of pseudo-purpurin compared to the other extracts. In the ethanolic extract, the predominant anthraquinone compound is lucidin primeveroside, indicating a distinct chemical profile. Among the three extracts, the methanol extract exhibits the highest overall anthraquinone content, suggesting that methanol is the most effective solvent for extracting these compounds.

When evaluating the extracts in terms of their phenolic compound content, the water extract contains the highest concentrations of gallic acid (1) and protocatechuic acid (2), making it particularly rich in these bioactive compounds. However, when considering phenolic compound diversity, the methanol extract stands out, as it contains the widest variety of phenolic compounds. This suggests that methanol is more efficient at extracting a broader range of phenolic compounds compared to water and ethanol.

3.2. Characterization of p(Rt) Particles

In Figure 4, $p(Rt)_m$, $p(Rt)_e$ and $p(Rt)_w$ particles, and SEM images were given. $p(Rt)_m$, $p(Rt)_e$ and $p(Rt)_w$ particles were prepared by a one-step emulsion polymerization technique. As observed in the SEM images, Rt particles exhibit a strong tendency to aggregate due to their extremely small size. This aggregation occurs because the high surface area of these tiny particles leads to increased interparticle attraction forces, such as van der Waals interactions. As multiple particles cluster together, the surface roughness of the aggregates becomes more pronounced, which can be clearly seen in the SEM images. This rough texture may influence the physical and chemical properties of the particles, potentially affecting their behavior in various applications. The strength of the zeta potential gives information about the stability of the system. If all particles in the system have a negative or positive zeta potential, they repel each other and stabilize the system. On the other hand, particles with low zeta potential do not have enough force to repel each other. Therefore, they come together to form lumps. The zeta potentials of p(Rt)e, p(RT)m, and p(Rt)w particles were -31.6 mV, 0.00567 mV, and -0.239 mV, respectively. The hydrodynamic diameters of

the synthesized p(Rt)e, p(RT)m, and p(Rt)w particles were 0.000162 nm (0.162 pm), 0.00023 nm (0.23 pm) and 0.000566 nm (0.523 pm), respectively.

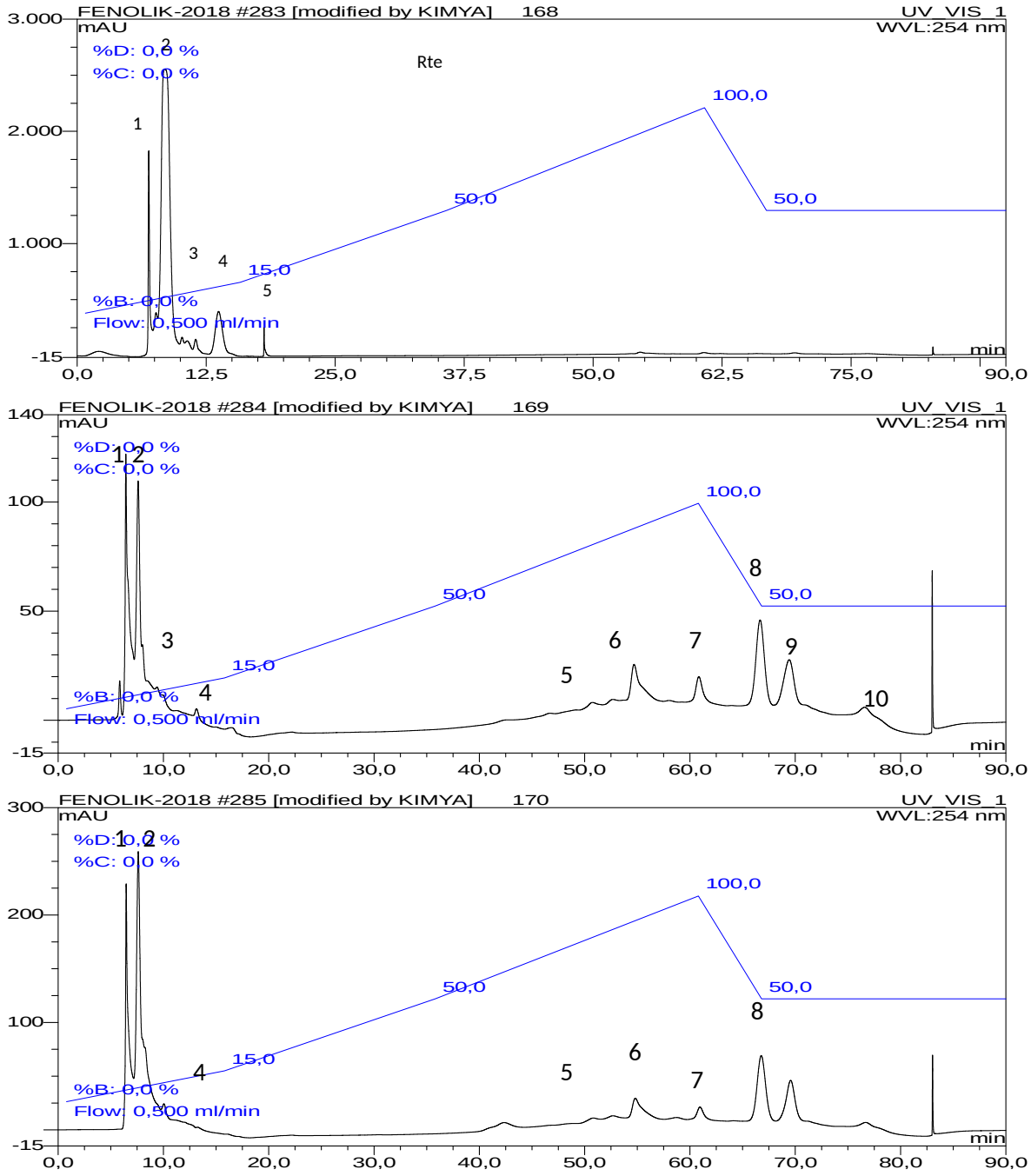

Figure 2. HPLC graph of phenol in Rt extract

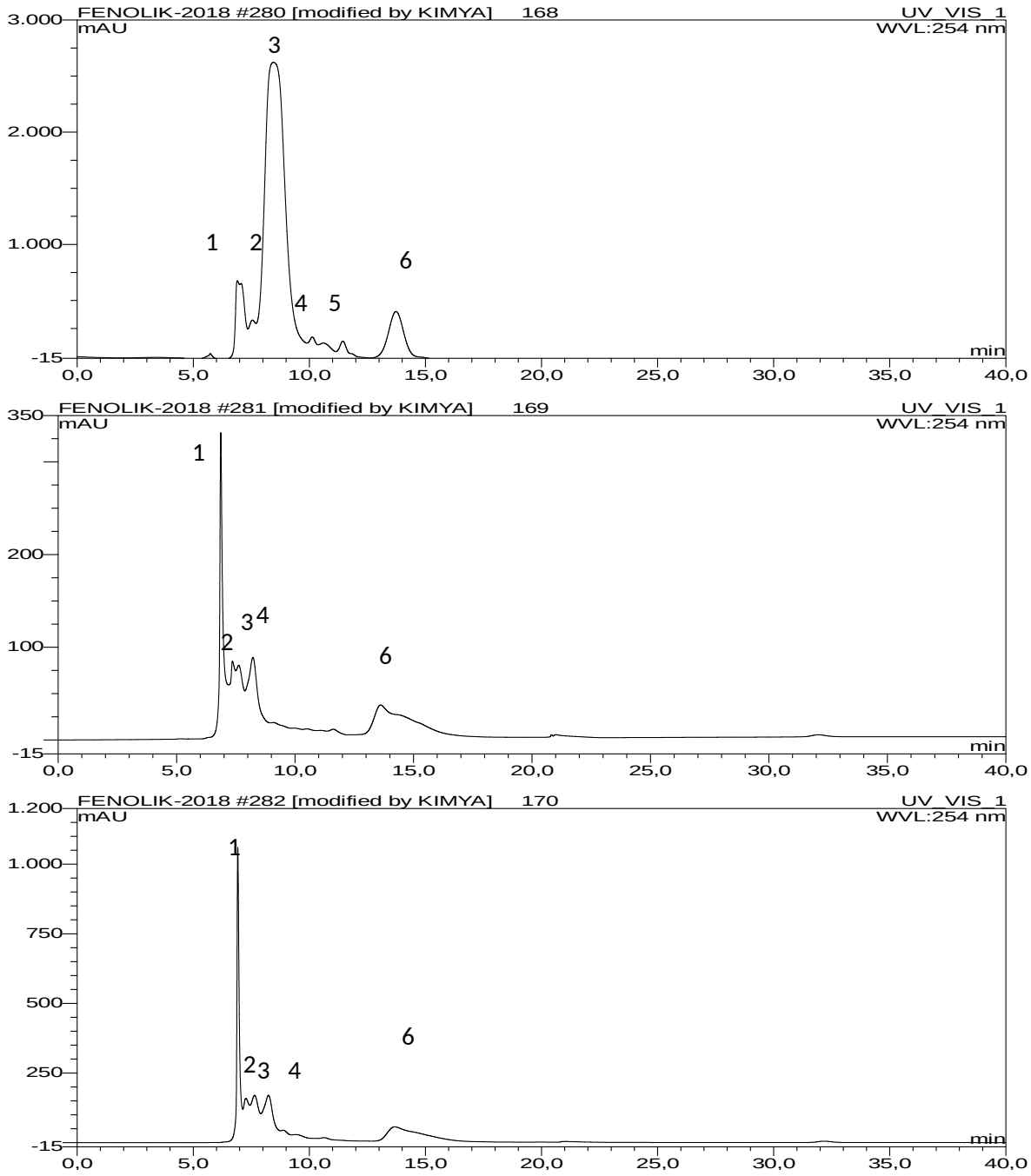

Figure 3. HPLC graph of anthraquinones in Rt extract

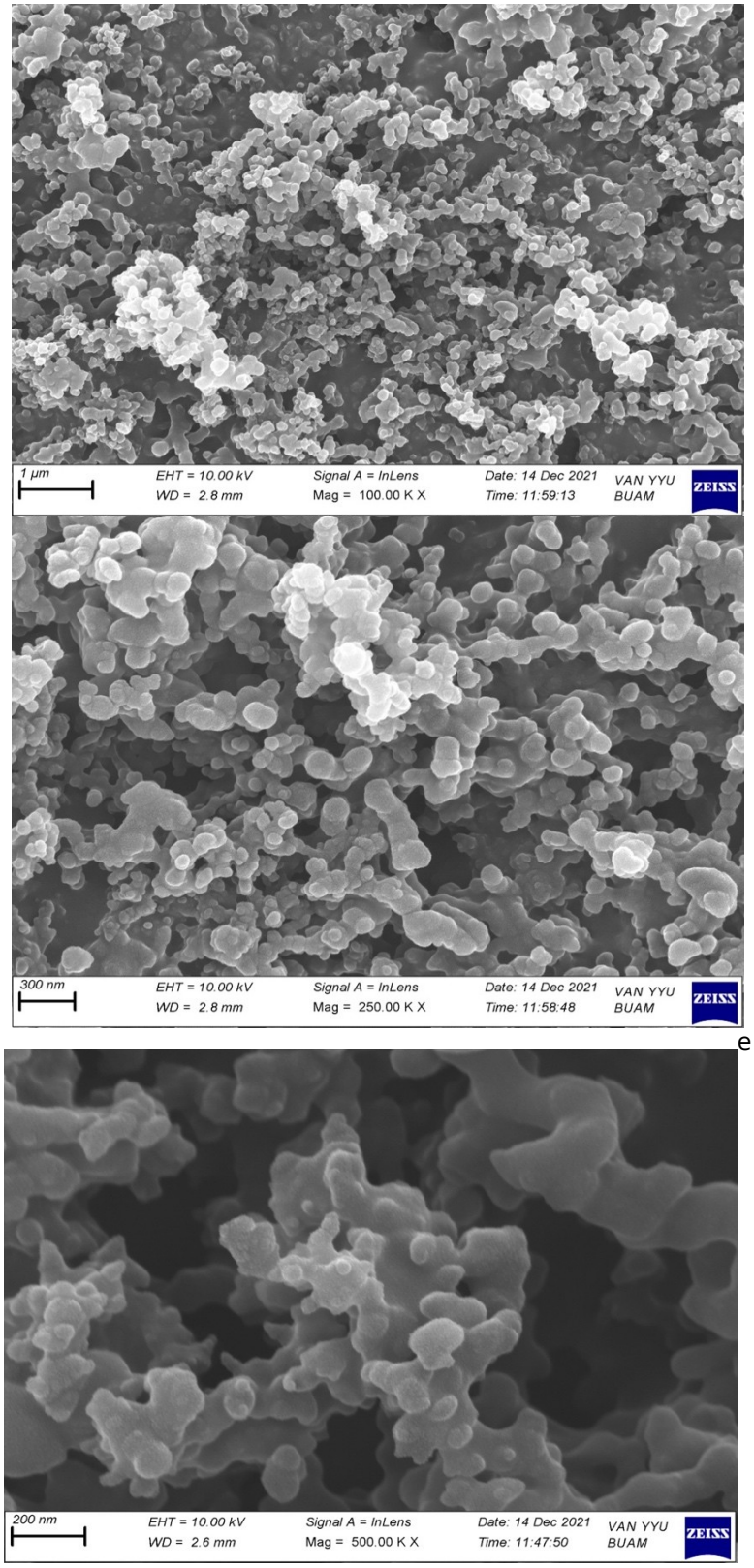

Figure 4. SEM image of p(Rt)w, p(Rt)e, p(Rt)m particles.

FT-IR spectrum from *Rubia tinctorum L.* shows peaks at 3424 cm^{-1} (OH), 2924 cm^{-1} (C– H), 1718 cm^{-1} (CO), 1636 cm^{-1} (C=C), 1285 cm^{-1}. The vibrational (C–O), 1054 cm^{-1} (C–O–C) and 815 cm^{-1} (O–H) were associated with polyols, carbonyl, and C=C bonds and indicate the presence of flavonoids and terpenoids in the extract. The bands at 2946 cm^{-1}, 2356 cm^{-1}, 1724 cm^{-1}, 1616 cm^{-1}, 1450 cm^{-1}, 1097 cm^{-1}, and 1145 cm^{-1} in Figure 5, showed the presence of active functional groups in the particle. It shows that the bands at 2928 cm^{-1} and 2851 cm^{-1} originate from aliphatic C–H stretching frequencies. The stretch band observed at 1724 cm^{-1} was the characteristic C=O ester group peak of the EGDMA crosslinker. The presence of the carbonyl group and amine indicated the stretch band at 1616 cm^{-1}. The FTIR band observed at 1450 cm^{-1} was defined as the C–C group containing aromatic C–H group/heteroatom and the band observed at 1100-1150 cm^{-1} was defined as the C-O-C group. Absorption bands characteristic for phenolic compounds, including anthracene derivatives, were observed at 1400-1200 cm^{-1}. FTIR peaks were associated with vibrational bands, polyols, carbonyl, and C=C bonds and indicate the presence of flavonoids and terpenoids from *Rubia tinctorum L.* extracts.

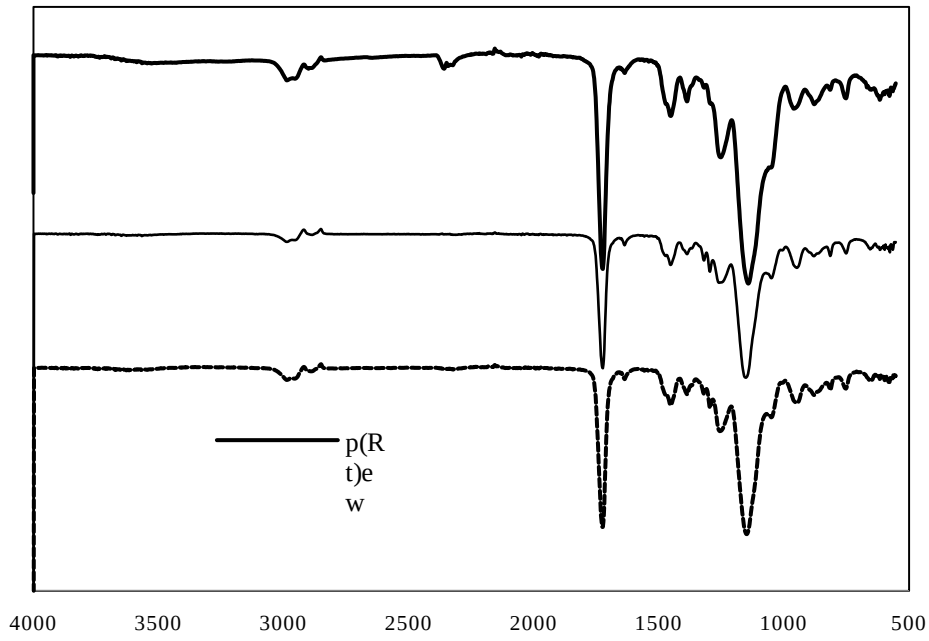

Figure 5. FT-IR spectra of p(Rt)w, p(Rt)e, p(Rt)m part.

3.3. Blood Compatibility Activity

According to the data obtained from the studies, the p(Rt) particles we synthesize were considered hemocompatible and biocompatible. If hemolysis values are less than 5%, it is considered hemocompatible, and between 5% and 10% is considered biocompatible (Belanger and Marois, 2001; Liu et al., 2014). When the hemolysis values of Rt_m extract and p(Rt)m particles in Figure 6 were examined, it was seen that blood cells were not affected. This demonstrates the usability of the methanol extract of *Rubia tinctorum L.* and the $p(Rt)_m$ particle in the body. The extracts were found to be Rt_m^1 0.053%, Rt_m^2 0.042%, and Rt_m^3 0.053%. The hemolysis results of the particles, $p(Rt)_m^1$, $p(Rt)_m^2$ and $p(Rt)_m^3$, were found to be 0.059%, 0.059% and 0.067%, respectively. As a result of the hemolytic analysis, it was determined that the hemolysis values remained below 5%, indicating that $p(Rt)_m$, $p(Rt)_e$, and $p(Rt)_w$, as well as Rt_m, Rt_e, and Rt_w, are biocompatible. Additionally, it was observed that p(Rt)m particles, synthesized from *Rubia tinctorum* (Rt), retained their non-hemolytic properties even after polymerization, confirming that the polymerization process did not negatively impact their blood compatibility. Moreover, $p(Rt)_m$ particles demonstrated higher hemocompatibility compared to the Rt_m extract, suggesting that polymer-based formulations may enhance biocompatibility.

Another approach to assessing the blood compatibility of *Rubia tinctorum* L. extracts and p(Rt)w particles is the Blood Coagulation Index (BCI). The analysis revealed that *Rubia tinctorum* L. extracts and p(Rt) particles exhibited BCI values ranging between 3% and 7%. According to the results presented in Figure 6, it was concluded that Rt extracts, and p(Rt) particles are blood-compatible and biocompatible, further supporting their potential for biomedical applications.

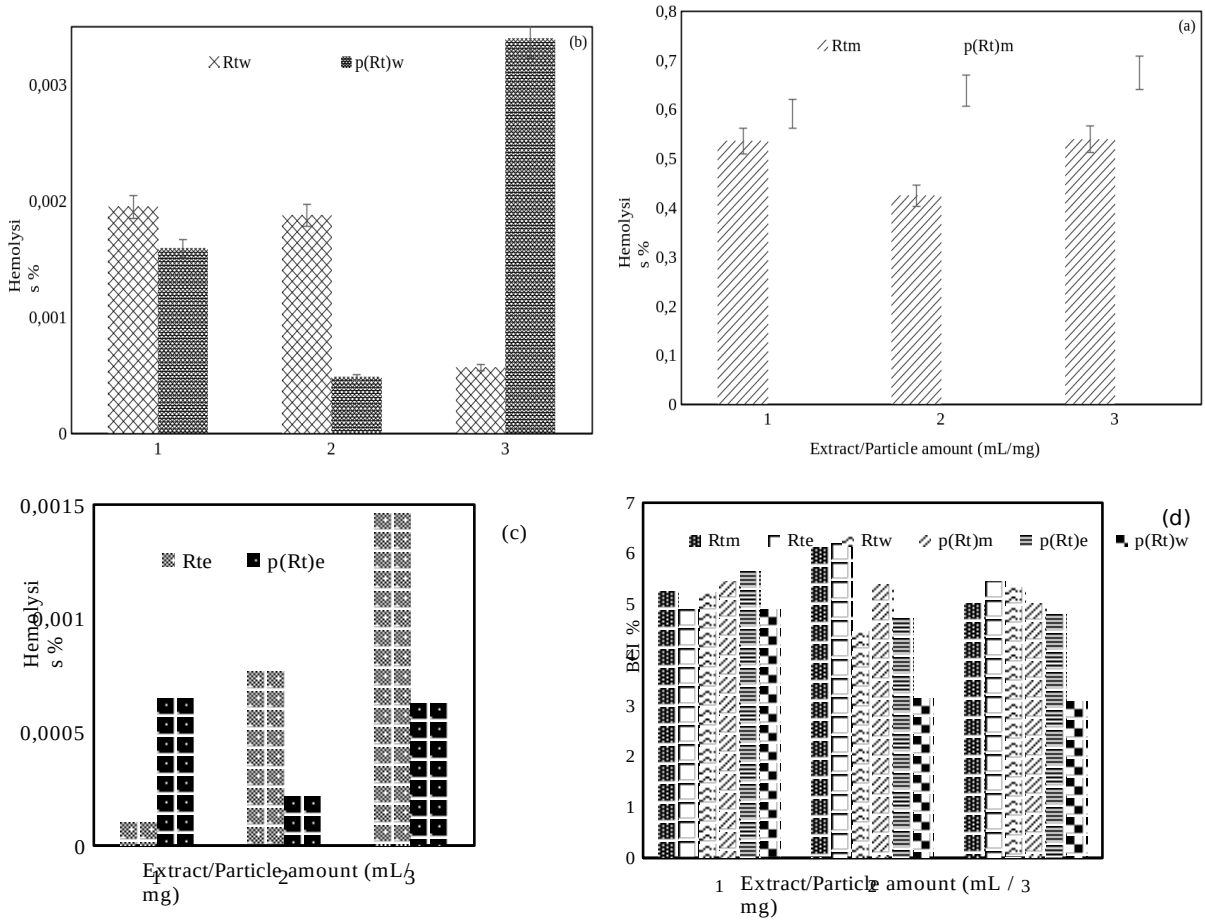

Figure 6. Hemolysis value of (a) $p(Rt)_m$, (b) $p(Rt)_w$ (c) $p(Rt)_e$ particles and (d) BCI index of $p(Rt)_m$, $p(Rt)_e$, $p(Rt)_w$ particles.

3.4. Antimicrobial Activity

When Figure 7 was examined, the antimicrobial capacities of Rt extracts and p(Rt) particles are determined against three Gram (+) (*Staphylococcus aureus, Bacillus cereus, Enterococcus faecalis*), two Gram (-) (*Escherichia coli, Pseudomonas aeruginosa*) bacteria and one yeast (*Candida albicans*) tested. It was determined that Rt_w extract has an antimicrobial effect against *S. aureus* and *C. albicans*; $p(Rt)_w$ particle had an antimicrobial effect against *B. cereus, S. aureus, E. faecalis* and *C. albicans*. It was determined that Rt_e extract has antimicrobial effects against *B. cereus, E. faecalis* and *C. albicans*. The $p(Rt)_e$ particle was found to have antimicrobial activity against *E. coli, B. cereus, S. aureus, E. faecalis*, and *C. albicans*. It was determined that the Rt_m extract was an antimicrobial effect against *B. cereus, S. aureus,* and *C. albicans*; the $p(Rt)_m$ particle showed an antimicrobial effect against *E. coli, B. cereus, S. aureus, E. faecalis* and *C. albicans*. These results are believed to be closely related to the intrinsic properties of the bioactive compounds, such as flavonoids and anthraquinones, present in the p(Rt)e, p(Rt)m, and p(Rt)w particles**.** Flavonoids and anthraquinones are well known for their antioxidant and antimicrobial properties, which may contribute to the observed effects. Moreover, previous studies have reported that *Rubia tinctorum* L. exhibits antimicrobial activity against various bacterial and fungal strains. This suggests that the presence of these bioactive compounds within the synthesized particles enhances their potential

for antimicrobial applications, further supporting their use in biomedical and pharmaceutical fields (Abachi et al., 2013; Manojlovic et al., 2005; Siva et al., 2011).

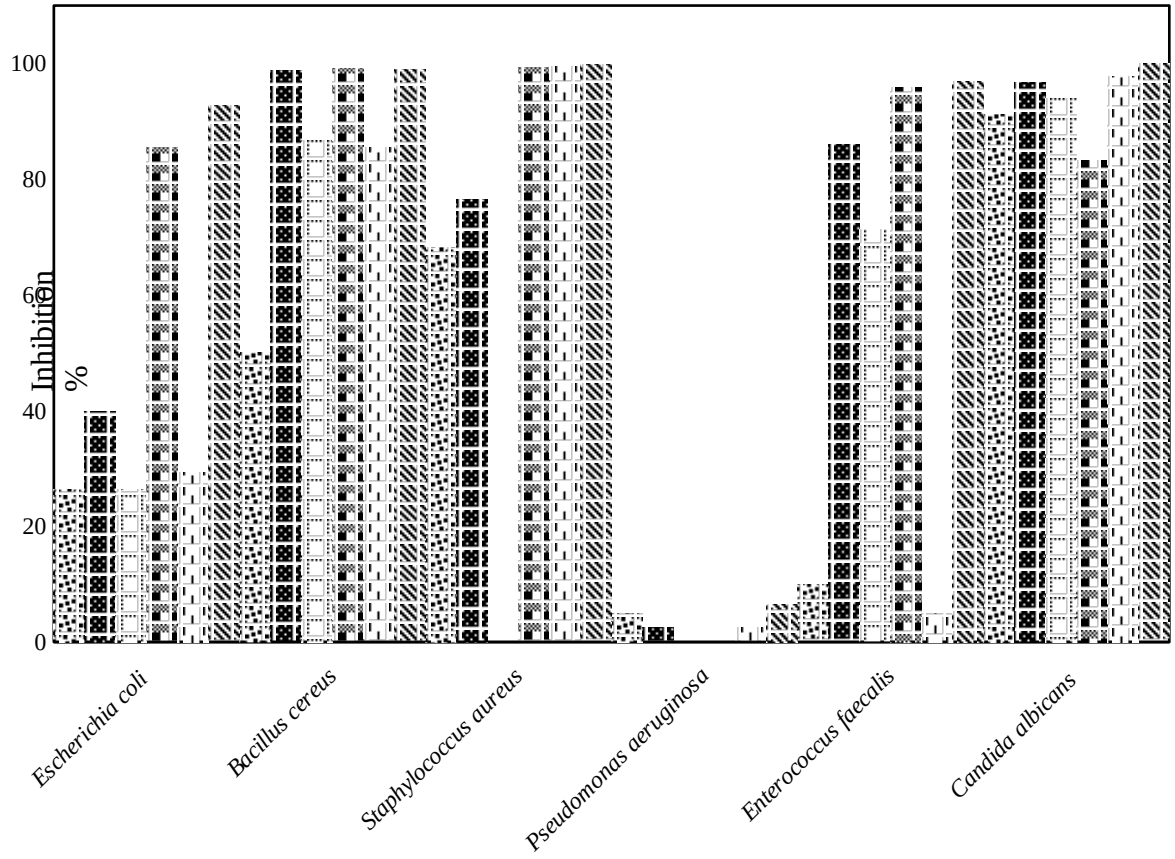

Figure 7. Antimicrobial activity of $p(Rt)_w$, $p(Rt)_e$, $p(Rt)_m$ particles.

3.5. Antioxidant Activity

The main components and roots of *Rubia tinctorum L.* are anthraquinones and flavonoids, which represent a large group of phenolic compounds. As seen in Table 1, it was observed that $p(Rt)_e$, $p(Rt)_m$ and $p(Rt)_w$ particles obtained from Rt also exhibited strong radical scavenging ability in a dose-dependent manner. The antioxidant activity of *Rubia tinctorum L.* extract is related to its phenolic content, especially anthraquinones and flavonoids. Hydroxyanthraquinones are more commonly found in medicinal plants than other natural quinones. Hydroxyanthraquinones normally have one to three hydroxyl groups in the anthraquinone structure (Cai et al., 2004; Mellado et al., 2013). There is a correlation between phenol, flavonoid, and alizarin contents and antioxidant activity. Alizarin belongs to the strongest anthraquinone antioxidant (Cai et al., 2004). For this reason, it is used as an antioxidant and colorant in foods (Jeremić et al., 2014). *Rubia tinctorum* species such as *R. cordifolia* contain a wide variety of antioxidants such as alizarin, hydroxyl anthraquinones, and rubiadin, which are used in various medicines. Total phenol content of Rt extracts in the literature, methanol extract of *Rubia tinctorum.* roots 118.38 ± 1.20 mg of gallic acid, *Rubia tinctorum L.* methanol extract 71.474±0.021 mg of gallic acid (Marhoume et al., 2021a), *Rubia tinctorum* ethanol extract 13.19 mg of gallic acid (Aşci et al., 2018) has been reported. The antioxidant activity of the synthesized p(Rt) particles in this study was found to be significantly higher than that of similar particles reported in the literature. This finding further confirms that the combination of antioxidants enhances overall effectiveness. Additionally, the p(Rt) particles exhibit strong antioxidant and antimicrobial properties, along with excellent biocompatibility. These characteristics make them promising candidates for applications in microorganism inhibition and infection prevention. Furthermore, their potential use in biomedical

fields, particularly as drug delivery materials, highlights their versatility, and potential impact in healthcare.

Table 1. Total phenol values.

Particles or Extracts	Particles Amount (mg) or Extract Amount (mL)	Total phenol (mg g^{-1})
p(Rt)e	10	70.7
p(Rt)e	20	100.7
p(Rt)e	30	134.7
Rte	10	45.5
Rte	20	86.2
Rte	30	92.1
p(Rt)m	10	7.3
p(Rt)m	20	12.1
p(Rt)m	30	55.1
Rtm	10	12.5
Rtm	20	18.4
Rtm	30	88.1
p(Rt)w	10	31.0
p(Rt)w	20	39.2
p(Rt)w	30	55.1
Rtw	10	31.8
Rtw	20	32.1
Rtw	30	49.2

3.6. Paracetamol and Ceftriaxone Release and Kinetics of Particles $p(Rt)_m$, $p(Rt)_e$ and $p(Rt)_w$

Drug release experiments of drug-loaded p(Rt) particles were performed by imitating the pH values of different parts of the body (stomach pH of 2, skin pH of 5.4, blood pH of 7.4 and intestinal pH of 8)(Alpaslan et al., 2022a; Ersen Dudu et al., 2021). Drug release experiments using drug-loaded p(Rt) particles were conducted by simulating the pH conditions of various physiologic environments in the body. These included the highly acidic conditions of the stomach (pH 2), the slightly acidic environment of the skin (pH 5.4), the neutral pH of blood (pH 7.4), and the mildly alkaline conditions of the intestine (pH 8). By evaluating drug release at these different pH levels, the study aimed to assess how effectively the p(Rt) particles respond to varying physiological conditions, providing insight into their potential for controlled and targeted drug delivery**.** Paracetamol and ceftriaxone drugs were chosen as model drugs to examine the drug release behavior of synthesized p(Rt) particles.

Figure 8 and Table 2 showed the paracetamol release behavior of drug-loaded $p(Rt)_e$, $p(Rt)_m$ and $p(Rt)_w$ particles at pH 2. When the graphs obtained were examined, it was seen that the release rates of paracetamol at pH 2 and pH 8 were fast at the beginning and slowed down after about 540 minutes. The highest cumulative paracetamol release amounts of $p(Rt)_m$, $p(Rt)_e$ and $p(Rt)_w$ particles were 76.5%, 68% and 61% at pH 2 and 91.17%, 83.67% and 83.67% at pH 8 (8640 min.). It was observed that the release of paracetamol by p(Rt) particles at pH 5.4 was fast at the beginning and slowed down after about 540 minutes. The highest cumulative Paracetamol drug release amounts of $p(Rt)_m$, $p(Rt)_e$ and $p(Rt)_w$ particles were 97.67%, 92.17% and 79.33%, respectively (the highest cumulative Paracetamol drug release rate was reached in 4320 min). At pH 7.4, however, the release of paracetamol slowed down after approximately 540 minutes and the highest cumulative Paracetamol drug release amounts of $p(Rt)_m$, $p(Rt)_e$ and $p(Rt)_w$ particles were 98% (8640 min) 95.50% (7200 min) and 68.83% (5760 min).

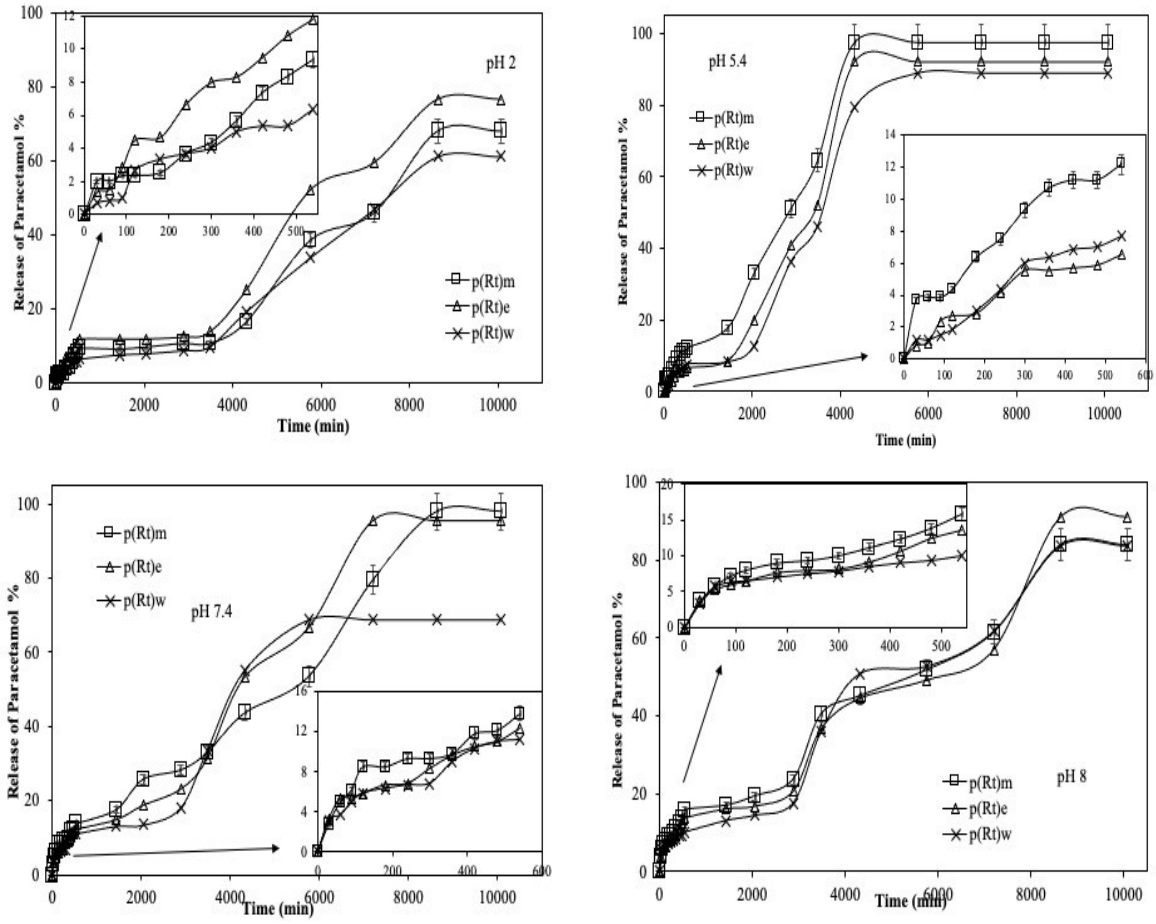

Figure 8. Release behavior of Paracetamol **(a)** 2.0 pHs **(b)** 5.4 pHs **(c)** 7.4 pHs **(d)** 8.0 pHs from particles.

Table 2. Release kinetic of Paracetamol and Ceftriaxone release

	Paracetamol			
	pH 2	pH 5	pH 7.4	pH 8
	% Release			
p(Rt)m	68.00	97.67	98.00	84.00
p(Rt)e	76.50	92.17	95.50	91.17
p(Rt)w	61.00	89.00	68.83	83.67
	Ceftriaxone			
	pH 2	pH 5	pH 7.4	pH 8
	% Release			
p(Rt)m	60.83	96.83	89.00	81.00
p(Rt)e	64.33	99.50	99.67	99.67
p(Rt)w	76.67	99.33	99.00	97.33

In Figure 9 and Table 2., ceftriaxone drug release behavior of particles at pH 2.0, 5.4, 7.4, 8.0 was shown. It was observed that the drug release from the particles was fast at the beginning and slowed down after about 540 minutes. The highest cumulative ceftriaxone drug release amount of $p(Rt)_m$, $p(Rt)_e$ and $p(Rt)_w$ particles were 76.56%, 64.33% and 60.83% (8640 min) at pH 2.0; 99.33% (8640 min), 99.50% (5760 min) and 96.83% (4320 min) at pH 5.4; 99.00% (8640 min), 99.67% (5760 min) and 89.00% (4320 min) at pH 7.4; 99.67%, 97.33% and 81.00% (8640 min) at pH 8.0, respectively.

Controlled drug release systems have a complex system and can be explained by many mathematical methods. In order to elucidate the mechanism of release of ceftriaxone and paracetamol drugs from drug-loaded particles, Zero Order Kinetic Model, First Order Kinetic Model, Korsmeyer-Peppas Model and Higuchi Models were applied. When the paracetamol releases kinetic models of $p(Rt)_m$, $p(Rt)_e$ and $p(Rt)_w$ particles were investigated in Table 3., the highest correlation coefficient value was found to be the Korsemeyer-Peppas model. In addition, constant velocity emission values of the Zeroth and First order kinetic models indicate that they are not suitable for these models. It was observed that the diffusion constant value ($n<0.5$) in the release of paracetamol fits the Fickian diffusion model at pH 7.4 and pH 8.0, the release is controlled by relaxation, and it was determined that it fits the non-Fickian diffusion model at pH 5.4 and pH 2.0 ($0.5<n<0.8$).

Table 3. Release kinetic of Paracetamol and Ceftriaxone release.

Paracetamol						Ceftriaxone					
p(Rt)m		**2.0**	**5.4**	**7.4**	**8.0**	**p(Rt)m**		**2.0**	**5.4**	**7.4**	**8.0**
ZoM	**Co**	0.006	0.052	0.088	0.093	**ZoM**	**Co**	0.0652	0.0135	0.0018	0.0425
	ko	0.0003	0.0004	0.0003	0.0004		**ko**	0.0003	0.0005	0.0006	0.0006
	R²	0.960	0.950	0.892	0.952		**R²**	0.8486	0.9822	0.9607	0.965
FoM	**Co**	2.517	2.409	2.105	2.344	**FoM**	**Co**	2.128	2.112	2.164	2.475
	k1	3.656	0.731	2.384	2.272		**k1**	2.479	3.556	3.528	2.686
	R²	0.923	0.879	0.744	0.852		**R²**	0.7554	0.7719	0.7719	0.9062
HM	**kh**	0.007	0.006	0.012	0.013	**HM**	**kh**	0.014	0.014	0.015	0.016
	R²	0.896	0.945	0.935	0.955		**R²**	0.8867	0.9965	0.9376	0.9369
KPM	**n**	0.732	0.703	0.395	0.396	**KPM**	**n**	0.413	0.937	0.958	0.671
	kkp	870.267	621.851	40.825	72.923		**kkp**	83.7386	897.847	735.095	340.84
	R²	0.896	0.988	0.925	0.950		**R²**	0.8411	0.9745	0.9824	0.9774
p(Rt)e		**2.0**	**5.5**	**7.4**	**8.0**	**p(Rt)e**		**2.0**	**5.4**	**7.4**	**8.0**
ZoM	**Co**	0.022	0.021	0.074	0.080	**ZoM**	**Co**	0.054	0.071	0.040	0.062
	ko	0.0004	0.0002	0.0003	0.0003		**ko**	0.0003	0.0004	0.0006	0.0006
	R²	0.978	0.921	0.976	0.957		**R²**	0.7852	0.8462	0.8807	0.9647
FoM	**Co**	27.023	38.986	11.914	10.947	**FoM**	**Co**	18.984	12.323	16.692	11.648
	k1	0.004	0.004	0.002	0.002		**k1**	0.0027	0.0027	0.0038	0.003
	R²	0.844	0.785	0.916	0.913		**R²**	0.6732	0.7452	0.7452	0.9177
HM	**kh**	0.006	0.006	0.015	0.013	**HM**	**kh**	0.012	0.006	0.009	0.012
	R²	0.948	0.963	0.960	0.933		**R²**	0.8973	0.8679	0.8707	0.9386
KPM	**n**	0.506	0.498	0.221	0.394	**KPM**	**n**	0.312	0.408	0.445	0.594
	kkp	177.541	340.495	12.739	91.442		**kkp**	54.055	160.244	164.828	261.465
	R²	0.971	0.960	0.670	0.918		**R²**	0.8854	0.9278	0.9051	0.9726
p(Rt)w		**2.0**	**5.5**	**7.4**	**8.0**	**p(Rt)w**		**2.0**	**5.4**	**7.4**	**8.0**
ZoM	**Co**	0.012	0.009	0.063	0.095	**ZoM**	**Co**	0.054	0.042	0.047	0.034
	ko	0.0002	0.0003	0.0003	0.0002		**ko**	0.0004	0.0004	0.0005	0.0004
	R²	0.944	0.951	0.960	0.883		**R²**	0.9096	0.9069	0.9547	0.6862
FoM	**Co**	55.936	38.271	13.572	10.345	**FoM**	**Co**	13.577	18.889	17.789	11.727
	k1	0.004	0.005	0.002	0.002		**k1**	0.003	0.004	0.004	0.002
	R²	0.800	0.858	0.911	0.745		**R²**	0.9411	0.8418	0.8553	0.6219
HM	**kh**	0.005	0.005	0.007	0.004	**HM**	**kh**	0.012	0.008	0.007	0.005
	R²	0.959	0.955	0.951	0.939		**R²**	0.9325	0.7882	0.7986	0.6821
KPM	**n**	0.554	0.863	0.474	0.474	**KPM**	**n**	0.526	0.721	0.694	0.694
	kkp	314.191	128.895	125.211	40.858		**kkp**	173.903	867.920	646.905	443.945
	R²	0.971	0.972	0.941	0.969		**R²**	0.8511	0.8856	0.9026	0.6904

It was determined that p(Rt)m, p(Rt)e and p(Rt)w particles obeyed the Korsemeyer-Peppas model, which is one of the ceftriaxone release kinetics models. It was observed that the diffusion constant value ($n<0.5$) of p(Rt)m particles obeyed Fickian diffusion at pH 2.0 and the release was controlled by relaxation. The diffusion constant value ($0.5<n<0.7$) was observed to obey the non-Fickian diffusion model at pH 8, indicating that the system was both diffusion and swelling controlled. In contrast, the release was diffusion controlled at pH 5.4 and pH 7.4 and its value was greater than 0.89. It was observed that the diffusion constant value (n) of p(Rt)e particles obeyed the Fickian diffusion model at pH 2.0, pH 5.4 and pH 7.4, and obeyed the non-Fickian diffusion model at pH 8.0. Since the diffusion constant (n) of p(Rt)w particles is between 0.5 and 0.7 at the applied pH values, the system is both diffusion and swelling controlled.

4. RESULT

This study presents the first synthesis and characterization of poly(Rubia tinctorum) (p(Rt)) particles derived from *Rubia tinctorum* L. extracts, demonstrating their potential as bioactive materials for controlled drug delivery. The successful polymerization of methanol, ethanol, and water extracts not only preserved but also enhanced the antioxidant, antimicrobial, and hemocompatibility properties of the plant's bioactive compounds. Additionally, the particles exhibited pH-responsive drug release behavior, making them promising candidates for targeted pharmaceutical applications.

Beyond drug delivery, the multifunctional properties of p(Rt) particles suggest their applicability in diverse fields, including cosmetics, medicine, energy, and environmental sciences. Future research should focus on in vivo biocompatibility studies, long-term stability assessments, and the potential for scaling up the synthesis process. Moreover, exploring the incorporation of additional therapeutic agents and evaluating the particles' effectiveness in various biomedical applications could further expand their utility.

This work establishes a foundation for the use of natural plant-derived polymers in modern drug delivery systems, paving the way for sustainable and biologically active materials in healthcare and beyond.

Conflict of interest: The authors declare that they have no conflict of interest. This research did not receive any specific funding.

Acknowledgments
This work is supported by the Van Yuzuncu Yıl University BAP with grant # FYL-2022-10034

References

Abachi, S., Khademi, F., Fatemi, H., & Malekzadeh, F. (2013). Study of antimicrobial activity of selected Iranian plant extracts on vancomycin resistant Staphylococcus epidermidis. *IOSR Journal of Dental and Medical Sciences*, *4*(1), 59–63.

Alpaslan, D. (2019). Use of colorimetric hydrogel as an indicator for food packaging applications. *Bulletin of Materials Science*, *42*(5), 247. https://doi.org/10.1007/s12034-019-1908-z

Alpaslan, D., Dudu, T. E., & Aktaş, N. (2018). Synthesis, characterization and modification of novel food packaging material from dimethyl acrylamide/gelatin and purple cabbage extract. *MANAS Journal of Engineering*, *6*(2), 110–128.

Alpaslan, D., Dudu, T. E., Şahiner, N., & Aktas, N. (2020). Synthesis and preparation of responsive poly(Dimethyl acrylamide/gelatin and pomegranate extract) as a novel food packaging material. *Materials Science and Engineering: C*, *108*, 110339. https://doi.org/10.1016/j.msec.2019.110339

Alpaslan, D., Ersen Dudu, T., & Aktas, N. (2022a). Agar and Sesame Oil Based Organo-Hydrogels as a Pharmaceutical Excipient in Paracetamol/Carboplatin Release Systems. *Indian Journal of Pharmaceutical Sciences*, *84*(2). https://doi.org/10.36468/pharmaceutical-sciences.929

Yavuzcanli, M., Alpaslan, D., Turan, A., & Ersen Dudu, T. (2025). *Journal of the Turkish Chemical Society Section B: Chemical Engineering*, *8*(2), 185–202.

Alpaslan, D., Ersen Dudu, T., & Aktas, N. (2022b). Evaluation of poly(agar-co-glycerol-co-castor oil) organo-hydrogel as a controlled release system carrier support material. *Polymer Bulletin*, *79*(8), 5901–5922. https://doi.org/10.1007/s00289-021-03777-9

Alpaslan, D., Erşen Dudu, T., & Aktas, N. (2023). Development of onion oil-based organo-hydrogel for drug delivery material. *Journal of Dispersion Science and Technology*, *44*(5), 750–762. https://doi.org/10.1080/01932691.2021.1974869

Alpaslan, D., Olak, T., Turan, A., Ersen Dudu, T., & Aktas, N. (2021). A garlic oil-based organo-hydrogel for use in pH-sensitive drug release. *Chemical Papers*, *75*(11), 5759–5772. https://doi.org/10.1007/s11696-021-01760-2

Alpaslan, D., Olak, T., Turan, A., Ersen Dudu, T., & Aktas, N. (2022). Use of Coconut Oil-Based Organo-Hydrogels in Pharmaceutical Applications. *Journal of Polymers and the Environment*, *30*(2), 666–680. https://doi.org/10.1007/s10924-021-02219-x

Aras Aşci, Ö., DemiRci, T., & Göktürk Baydar, N. (2018). Effects of NaCl applications on root growth and secondary metabolite production in madder (Rubia tinctorum L.) root cultures. *International Journal of Secondary Metabolite*, *5*(3), 210–216. https://doi.org/10.21448/ijsm.453016

Böhm, B. H. H. (1993). *Handbuch der Naturfarbstoffe*. Lech, Ecomed Verlagsgesellschaft.

Cai, Y., Luo, Q., Sun, M., & Corke, H. (2004). Antioxidant activity and phenolic compounds of 112 traditional Chinese medicinal plants associated with anticancer. *Life Sciences*, *74*(17), 2157–2184. https://doi.org/10.1016/j.lfs.2003.09.047

Childs, R. E., & Bardsley, W. G. (1975). The steady-state kinetics of peroxidase with 2,2′-azino-di-(3-ethyl-benzthiazoline-6-sulphonic acid) as chromogen. *Biochemical Journal*, *145*(1), 93–103. https://doi.org/10.1042/bj1450093

Derksen, G. C. H., Van Holthoon, F. L., Willemen, H. M., Krul, C. A. M., Franssen, M. C. R., & Van Beek, T. A. (2021). Development of a process for obtaining non-mutagenic madder root (Rubia tinctorum) extract for textile dyeing. *Industrial Crops and Products*, *164*, 113344. https://doi.org/10.1016/j.indcrop.2021.113344

Ersen Dudu, T., Alpaslan, D., & Aktas, N. (2022). Application of Poly (Agar-Co-Glycerol-Co-Sweet Almond Oil) Based Organo-Hydrogels as a Drug Delivery Material. *Journal of Polymers and the Environment*, *30*(2), 483–493. https://doi.org/10.1007/s10924-021-02212-4

Essaidi, I., Snoussi, A., Ben Haj Koubaier, H., Casabianca, H., & Bouzouita, N. (2017). Effect of acid hydrolysis on alizarin content, antioxidant and antimicrobial activities of *Rubia tinctorum* extracts. *Pigment & Resin Technology*, *46*(5), 379–384. https://doi.org/10.1108/PRT-11-2015-0116

Gilbert, K. G., & Cooke, D. T. (2001). Dyes from plants: Past usage, present understanding and potential. *Plant Growth Regulation*, *34*(1), 57–69. https://doi.org/10.1023/A:1013374618870

Jeremić, S., Filipović, N., Peulić, A., & Marković, Z. (2014). Thermodynamical aspect of radical scavenging activity of alizarin and alizarin red S. Theoretical comparative study. *Computational and Theoretical Chemistry*, *1047*, 15–21. https://doi.org/10.1016/j.comptc.2014.08.007

Korsmeyer, R. W., Gurny, R., Doelker, E., Buri, P., & Peppas, N. A. (1983). Mechanisms of solute release from porous hydrophilic polymers. *International Journal of Pharmaceutics*, *15*(1), 25–35. https://doi.org/10.1016/0378-5173(83)90064-9

Manojlovic, N. T., Solujic, S., Sukdolak, S., & Milosev, M. (2005). Antifungal activity of Rubia tinctorum, Rhamnus frangula and Caloplaca cerina. *Fitoterapia*, *76*(2), 244–246.

Yavuzcanli, M., Alpaslan, D., Turan, A., & Ersen Dudu, T. (2025). *Journal of the Turkish Chemical Society Section B: Chemical Engineering*, *8*(2), 185–202.

Marhoume, F. Z., Aboufatima, R., Zaid, Y., Limami, Y., Duval, R. E., Laadraoui, J., Belbachir, A., Chait, A., & Bagri, A. (2021). Antioxidant and Polyphenol-Rich Ethanolic Extract of Rubia tinctorum L. Prevents Urolithiasis in an Ethylene Glycol Experimental Model in Rats. *Molecules*, *26*(4), 1005. https://doi.org/10.3390/molecules26041005

Marsoul, A., Boukir, A., Ijjaali, M., Taleb, M., Arrousse, N., Salim, R., & Dafali, A. (2023). Phytochemical Characterization, Antioxidant Proprieties and Electrochemical Investigations of Methanolic Extract of Rubia t.L. Roots for LC-Steel Corrosion Protection in 1 M HCl Medium. *Journal of Bio- and Tribo-Corrosion*, *9*(2), 32. https://doi.org/10.1007/s40735-023-00749-6

Mellado, M., Madrid, A., Peña-Cortés, H., López, R., Jara, C., & Espinoza, L. (2013). ANTIOXIDANT ACTIVITY OF ANTHRAQUINONES ISOLATED FROM LEAVES OF MUEHLENBECKIA HASTULATA (J.E. SM.) JOHNST. (POLYGONACEAE). *Journal of the Chilean Chemical Society*, *58*(2), 1767–1770. https://doi.org/10.4067/S0717-97072013000200028

Olak, T., Turan, A., Alpaslan, D., Dudu, T. E., & Aktaş, N. (2020). Developing poly(Agar-co-Glycerol-co-Thyme Oil) based organo-hydrogels for the controlled drug release applications. *Journal of Drug Delivery Science and Technology*, *60*, 102088. https://doi.org/10.1016/j.jddst.2020.102088

Orban, N., Boldizsar, I., Szucs, Z., & Danos, B. (2008). Influence of different elicitors on the synthesis of anthraquinone derivatives in Rubia tinctorum L. cell suspension cultures. *Dyes and Pigments*, *77*(1), 249–257. https://doi.org/10.1016/j.dyepig.2007.03.015

Ozdemir, M. B., & Karadag, R. (2023). Madder (*Rubia tinctorum* L.) as an Economic Factor Under Sustainability Goals in the Textile Dyeing. *Journal of Natural Fibers*, *20*(1), 2128968. https://doi.org/10.1080/15440478.2022.2128968

Ruch, R. J., Cheng, S., & Klaunig, J. E. (1989). Prevention of cytotoxicity and inhibition of intercellular communication by antioxidant catechins isolated from Chinese green tea. *Carcinogenesis*, *10*(6), 1003–1008. https://doi.org/10.1093/carcin/10.6.1003

Singleton, V. L., & Rossi, J. A. (1965). Colorimetry of Total Phenolics with Phosphomolybdic-Phosphotungstic Acid Reagents. *American Journal of Enology and Viticulture*, *16*(3), 144–158. https://doi.org/10.5344/ajev.1965.16.3.144

Siva, R., Palackan, M. G., Maimoon, L., Geetha, T., Bhakta, D., Balamurugan, P., & Rajanarayanan, S. (2011). Evaluation of antibacterial, antifungal, and antioxidant properties of some food dyes. *Food Science and Biotechnology*, *20*(1), 7–13. https://doi.org/10.1007/s10068-011-0002-0

Swain, T. (1966). *Comparative phytochemistry. 43*, 1791.

Zohra, H. F., Ramazan, E., & Ahmed, H. (2022). Biological activities and chemical composition of rubia tinctorum (l) root and aerial part extracts thereof. *Acta Biológica Colombiana*, *27*(3), 403–414.

Yavuzcanli, M., Alpaslan, D., Turan, A., & Ersen Dudu, T. (2025). *Journal of the Turkish Chemical Society Section B: Chemical Engineering*, *8*(2), 185–202.